Solvent Extraction Research and Development, Japan, **Vol. 29, No 1, 9 – 19 (2022)**

Ultrasound-Assisted Micro-Channel Extraction of Magnesium from Wet-Process Phosphoric Acid

Qi XIA[1], Jiangpo ZHANG[1], Xiaofeng HONG[1], Jianjun CHEN[1,2,*] and Daijun LIU[1,2]

[1]School of Chemical Engineering, Sichuan University, Chengdu 610065, China; [2]Engineering Research Center for Comprehensive Utilization and Cleaning Process of Phosphate Resource, Ministry of Education, Chengdu 610065, China

(Received January 20, 2021; Accepted March 29, 2021)

A new extractant PN-1 was synthesized, and an ultrasound-assisted micro-channel extraction (UAME) system was developed for the extraction of magnesium from wet-process phosphoric acid (WPA). The effects of O/A ratio, P_2O_5 content, initial pH, ultrasound power, and aqueous phase ratio on extraction were investigated. The extraction efficiency of Mg^{2+} could reach 89.09% under the conditions of 74 W ultrasound power, 4 O/A ratio, and 0.2 mL/min aqueous phase velocity. The response surface methodology (RSM) result indicated that O/A ratio and aqueous phase velocity have extremely significant influences on extraction efficiency, significant interaction existed between ultrasound power and aqueous phase velocity, and ultrasound power evidently reduced extraction time. Furthermore, the magnesium could be fully stripped by 1 mol/L H_2SO_4 with a phase ratio lower than 2. Thus, the new extractant PN-1 and ultrasound-assisted micro-channel extraction system are suitable for the extraction of magnesium from wet-process phosphoric acid.

1. Introduction

Phosphoric acid is the primary feedstock of daily consumption products such as fertilizer, medicine, and food [1]. Usually, commercial phosphoric acid is produced via hot-process or wet-process. And due to the low-cost and low-energy advantages of the wet-process, 90% of phosphoric acid is produced through the wet-process [2-4]. However, many impurities are introduced into WPA (wet-process phosphoric acid) production, and Mg may be the most annoying impurity because it can increase the viscosity of WPA [4-6]. Therefore, Mg must be removed from WPA before subsequent application. Many methods have been proposed to remove Mg from WPA, such as ion exchange [7,8], membrane separation [9-11], chemical precipitation [12,13], and solvent extraction [4,14-17]. Recently, solvent extraction has increasingly drawn attention for its high separation efficiency and reasonable cost [18].

Mass transfer is the most critical issue affecting the extraction. As a mass transfer enhancement extraction technique, ultrasound-assisted extraction (UAE) was reported to show shorter extract time, lower energy consumption, and usage of the extractant, which owes to the acoustic effect and ultrasound cavitation phenomenon [19-24]. Microreactors are widely used in fields ranging from the rare earth to the food industry [25,26]. In addition, microfluidic solvent extraction has drawn much attention in the last decade. In a typical microfluidic reactor like the micro-channel, the organic phase and aqueous phase are limited in a specific space, leading to the enhancement of the mass transfer because of the significant increase of interface area

and contact opportunity [27-30]. In our previous work, the extractant D2EHPA had shown great efficiency for the extraction of Fe^{3+} in the UAME system [2,3]. However, D2EHPA showed less efficiency when dealing with Mg^{2+} in WPA. Hence, a more comprehensive study in the extraction of Mg^{2+} from WPA was still needed.

In this paper, a new extractant was synthesized and used to extract magnesium from WPA in an ultrasound-assisted micro-channel device designed by ourselves. In UAME, the extraction conditions of P_2O_5 content, initial pH, aqueous phase ratio, ultrasound power, and O/A ratio were studied in detail. The interactions between conditions were further analyzed using RSM. In addition, the following stripping process of magnesium was also studied to test the reusability of the extractant.

2. Experimental

2.1 Reagents

The aqueous phase (WPA) was simulated by dissolving the right amount of magnesium sulfate (10 g/L Mg^{2+}) into phosphoric acid (20% P_2O_5). Ammonium hydroxide, magnesium sulfate, phosphorus oxychloride, and phosphoric acid were purchased from Kelong Chemical Co (Sichuan, China) (AR grade). Polyol, a kind of mixed alcohol with an average molecular weight of 185, was purchased from Kelong Chemical Co (Sichuan, China). Sulfonated kerosene was provided by Zhongcui Chemical Co. (Sichuan, China). All the reagents were used without further purification.

2.2 Synthesis of extractant PN-1

PN-1 was prepared as following: 50 g phosphorus oxychloride and 90 g polyol reacted in a water bath at 50 ℃ for 8 hours. Then 100 mL water was added and kept at 80 ℃ for 4 hours. The oil phase was separated in a rotary evaporator in vacuum then reacted with ammonium hydroxide at room temperature for 30 min to acquire PN-1 with a density of 0.993 g/mL and viscosity of 51.3 mPa·s.

2.3 Extractions with micro-channel and ultrasound

The extraction efficiency was evaluated in a microchannel device equipped with an ultrasound generator, as shown in Figure S1. The extractant and aqueous phase were injected in two independent channels by syringe pumps at different velocities, and the organic phase velocity was set by multiplying the values of O/A ratio and aqueous phase velocity. Then mixing phase flowed through the entire micro-channel. The outlet fluid was collected in a separatory funnel. Then the aqueous phase was acquired for testing.

2.4 Experiment design and modeling

According to the results of single-factor experiments, response surface methodology (RSM) was adopted to investigate the synergistic effect of independent variables (aqueous phase velocity X_1, ultrasound power X_2, O/A ratio X_3). The variable aqueous phase velocity was set to acquire different residence times. And a Box-Behnken design (BBD) with three independent variables at three levels was then performed. The full data is shown in Table S1.

The observed response and data were fitted into a quadratic model. The regression model of the response given by an equation is presented in the generalized form:

$$Y = \alpha_0 + \sum_{i=1}^{3} \alpha_i X_i + \sum_{i=1}^{3} \alpha_{ii} {X_i}^2 + \sum_{i<j}^{3} \alpha_{ij} X_i X_j \quad (1)$$

where Y is the predicted response, α_0 is a constant, α_0, α_{ii} and α_{ij} are the linear, quadratic, and interactive coefficients, respectively. X_i and X_j are independent variables.

2.5 The determination of the extraction efficiency

The concentration of Mg^{2+} in the aqueous phase was determined by the ICP-OES method through an optima 7000DV from PerkinElmer company. All data in this paper are the even values based on two independent measurements, and the extraction efficiency can be calculated through Equation (2):

$$E = \frac{C_{aq}^{i}V_{aq}^{i} - C_{aq}^{r}V_{aq}^{r}}{C_{aq}^{i}V_{aq}^{i}} \times 100\% \quad (2)$$

where E is the extraction efficiency, the $C_{aq}{}^{i}$ is the Mg^{2+} concentration of the initial aqueous phase; $V_{aq}{}^{i}$ is the volume of that phase; $C_{aq}{}^{r}$ is the Mg^{2+} concentration of the extraction raffinate (the remaining aqueous phase); $V_{aq}{}^{r}$ stands for the raffinate volume.

3. Result and discussion

3.1 Effect of P_2O_5 content

The effect of P_2O_5 content in the aqueous phase on extraction efficiency was studied under the following conditions: different O/A ratios and aqueous phase velocity of 0.1 mL/min. The results are presented in Figure 2.

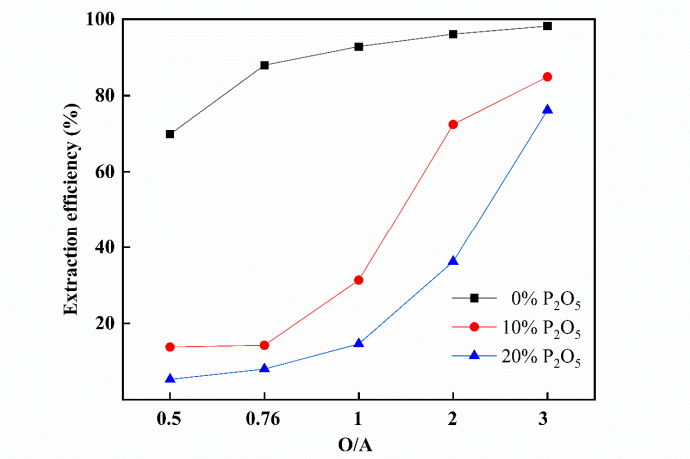

Figure 1. Effect of P_2O_5 content on extraction efficiency.

As shown in Figure 1, at the same O/A ratios, the extraction efficiency of magnesium decreased when the P_2O_5 content increased from 0% to 20%. In addition, in 0% P_2O_5 content, the extraction efficiency of magnesium still maintained at a high level even at the low O/A ratios. The result indicates that P_2O_5 content has a marked inhibitory effect on the extraction of magnesium. The influence could be explained by the interaction strength between cations and ligands, which could be predicted through a model called hard and soft acid base (HSAB) [31,32]. The extraction process could be expressed by Equation (3):

$$Mg^{2+} + 2NH_4A \rightleftharpoons MgA_2 + 2NH_4{}^{+} \quad (3)$$

where NH_4A is PN-1, as the A^- of PN-1 could be regarded as a hard base, and H^+, Mg^{2+}, $NH_4{}^+$ could be regarded as hard acid. Base on the HSAB principle, stable complexes could form between those acids and bases. And according to I.D. Brow's theory, the sequence of Lewis Acid strengths is $H^+ > Mg^{2+}$, which means that the stability of the formed complexes should be HA > MgA_2 [31,33]. As the extraction with 0% P_2O_5 content in Figure 2 had the best capacity of magnesium, it could be explained as the less amount of H^+ ions caused an effortless replacement between Mg^{2+} and $NH_4{}^+$, which had made the efficiency increased sharply.

However, the curves of 10% and 20% P_2O_5 content are different. The reason is a more stable complex formed between H^+ and R^-, which had decreased the extraction efficiency of magnesium.

3.2 Effect of initial pH

To further investigate the effect of H^+ ions, the effect of initial pH was studied under the following conditions: O/A ratio of 0.5, aqueous phase velocity of 0.1 mL/min, 0% P_2O_5 content.

As shown in Figure 2, the extraction efficiency increased with the initial pH value increasing at a lower range (pH<2.5), then held constant (pH≥2.5). The data shows a large increasing amount of H^+ ions at low initial pH inhibited the extraction of Mg^{2+} ions. The result is consistent with section 3.1 that a stable complex of HA was formed first when there were not enough extractants.

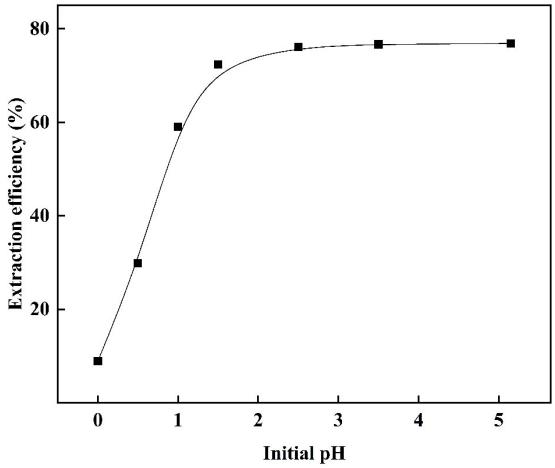

Figure 2. Effect of initial pH on extraction efficiency.

3.3 Effect of aqueous phase velocity

The effect of aqueous phase velocity on extraction efficiency was studied under the following conditions: O/A ratio of 2, 20% P_2O_5 content. The results are presented in Figure 3.

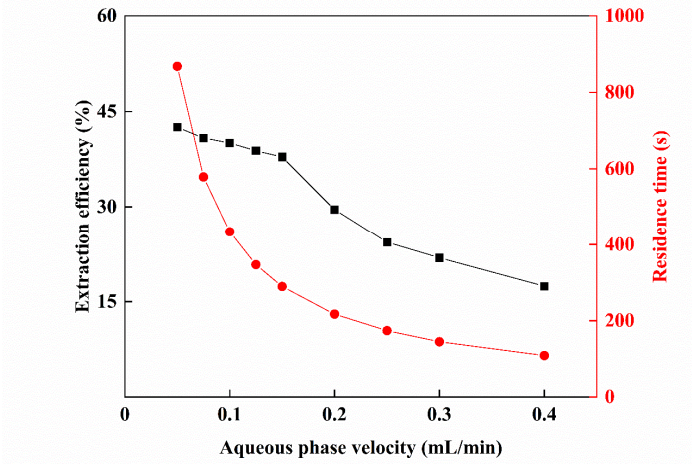

Figure 3. Effect of aqueous phase velocity on extraction efficiency.

As shown in Figure 3, the extraction efficiency decreased sharply from 42.52% to 17.41%, with residence time from 868 s to 108 s. However, when the aqueous phase velocity was less than 0.15 mL/min, there was no apparent decrease in efficiency. For aqueous phase velocity higher than 0.2 mL/min, the

efficiency quickly dropped with decreased residence time. The result indicated that the longer residence time provided sufficient mass transfer and facilitated the extraction of magnesium in the UAME method.

3.4 Effect of O/A ratio

The effect of O/A ratio was studied under the following conditions: different aqueous phase velocities of 0.05 mL/min to 0.3 mL/min, 20% P_2O_5 content.

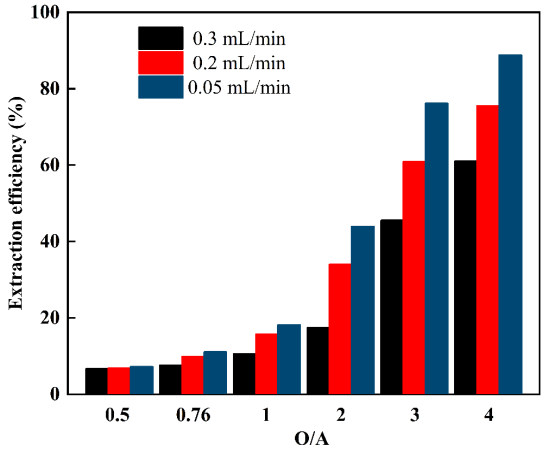

Figure 4. Effect of O/A ratio on extraction efficiency.

As shown in Figure 4, at all three aqueous phase velocities, the extraction efficiency increased with O/A ratio, and the gaps of efficiency between those velocities were small at low O/A ratios. However, when the O/A ratios were higher than 2, the extraction efficiency of 0.05 mL/min was much higher than that of 0.2 mL/min or 0.3 mL/min, which indicates that a high O/A ratio must work with a more extended residence to facilitate the extraction. For 0.05 mL/min aqueous phase velocities, the extraction efficiency increased with the O/A ratio from 0.5 to 4 and reached a high extraction efficiency of 88.84%. The high efficiency may be attributed to the merit of micro-channel, which is illustrated in Figure S2. In the micro-channel extraction, the mixing phase under high O/A ratios could be regarded as a reaction unit. The interface to volume ratio was increased from 70.69 m^2/m^3 to 1728.19 m^2/m^3 when comparing with the conventional batchwise method. In each unit, the liquid-liquid interfacial area was sufficient to ensure mass transfer. Therefore, plenty of extractants could contact and react with the magnesium ion, improving the extraction efficiency.

3.5 Effect of ultrasound power

The effect of ultrasound power was studied in different aqueous phase velocities and different O/A ratios with 20% P_2O_5 content.

As shown in Figure 5, the extraction efficiency increased with the increasing ultrasound power when the aqueous velocities were 0.2 mL/min and 0.3 mL/min. At an O/A ratio of 4, there is an apparent increase of efficiency from 60.94% to 76.75% in 0.3 mL/min with 74 W ultrasound power. In addition, the efficiency increase was also displayed in 0.2 mL/min from75.49% to 89.09% in the same conditions, maintained at the same efficiency level as 0.05 mL/min, which indicates that the ultrasound had promoted the mass transfer. The high ultrasound power had made up for the lack of residence time in UAME in high aqueous velocities.

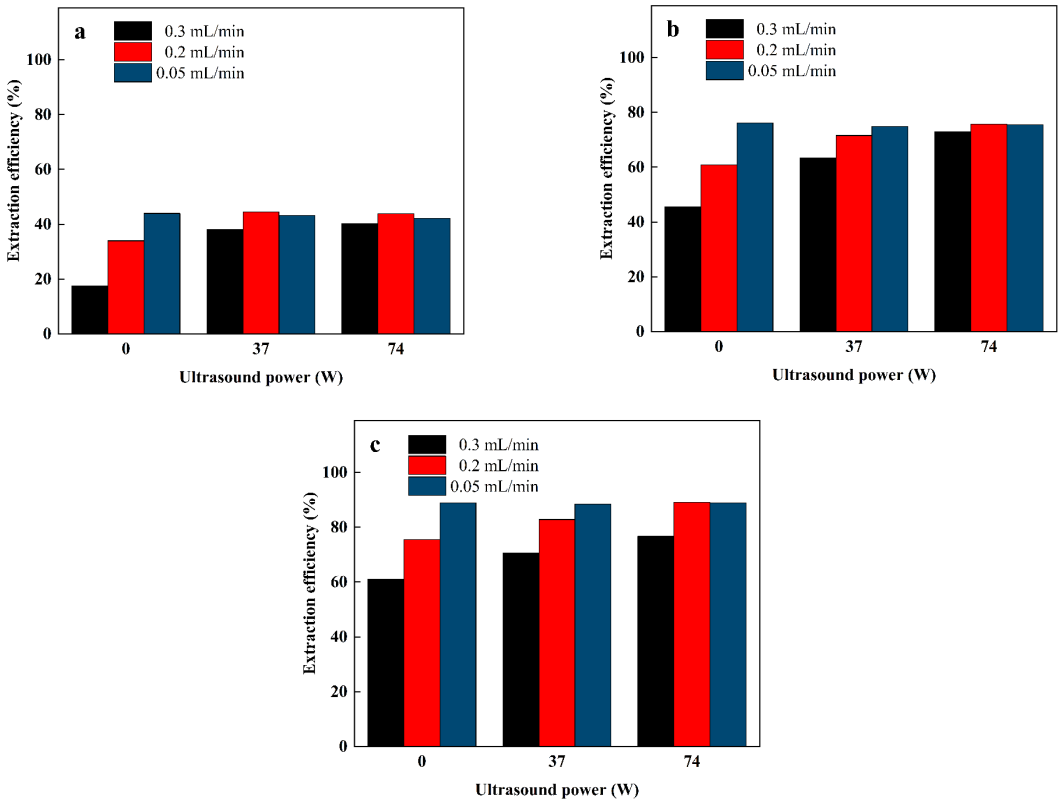

Figure 5. Effect of ultrasound power on extraction efficiency (a) O/A ratio=2; (b) O/A ratio=3; (c) O/A ratio=4.

3.6 Ultrasound on mass transfer intensity

To further study the influence of ultrasound power on mass transfer, a plot of ln $[(3C_{aq} - C_{aq0})/ 2C_{aq0}]$ versus residence time was presented in Figure 6. The mass transfer coefficient (k_p) was defined, which could be calculated by the following equations:

$$-\frac{dC_{aq}}{dt} = k_p(C_{aq} - C_{org}) \quad (4)$$

As the O/A ratio was 2, the concentration in organic phase could be calculated as:

$$C_{org} = (C_{aq0} - C_{aq})/2 \quad (5)$$

where C_{aq} and C_{aq0} is the concentration of Mg^{2+} in the aqueous phase at a certain time and at the initial time, respectively. The C_{org} is the concentration in organic phase. By integrating Equation. (4) and (5), the Equation. (6) is shown below:

$$\ln\left(\frac{3C_{aq}-C_{aq0}}{2C_{aq0}}\right) = -\frac{3}{2}k_p t \quad (6)$$

The straight line shown in Figure 7 means that the mass transfer of magnesium in UAME fitted the first order kinetics model well, and the different slopes of these lines mean k_p increased with ultrasound power, and mass transfer was intensified. The improvement may come from the ultrasound effect on extraction, which is the liquid cavitation caused by ultrasonic waves, shown in Figure S3. The cavitation bubbles that were in the process of continuous production and closure, local high temperature, and pressure [20], caused turbulence in the fluid. The more turbulent the fluid was, the two phases were more likely to contact. Eventually, those phenomena enhanced the mass transfer process.

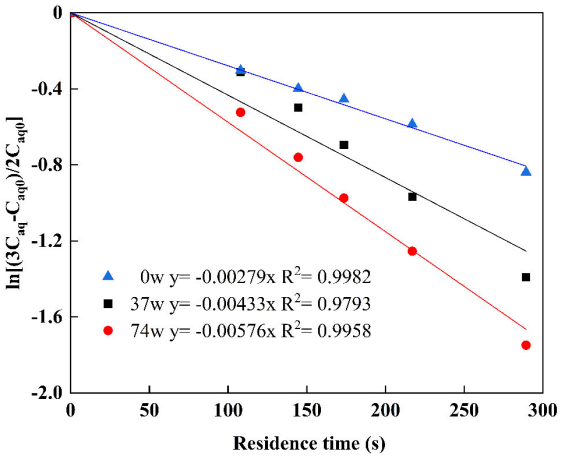

Figure 6. Different ultrasound power on mass transfer in UAME.

3.7 Model fitting and analysis

The BBD experiments of three independent variables were performed, and the observed responses (extraction efficiency) are shown in Table S1. The regression analysis of the response was carried out, and the quadratic polynomial equation gives the predicted model:

$$Y = -83.36 + 152.10X_1 + 0.20X_2 + 76.02X_3 + 1.74X_1X_2 - 28.66X_1X_3 - 0.02X_2X_3 - 581.04{X_1}^2 - 8.24{X_3}^2 \quad (7)$$

where X_1, X_2, X_3 are aqueous phase velocity, ultrasound power, and O/A ratio, respectively. Y is the predicted extraction efficiency.

Analysis of variance (ANOVA) was carried out to identify the adequacy of the developed model, and the analytical results were summarized in Table S2. The model F-value (16.27) and p-value (0.0007) shows that the regression equations could mostly represent the effect of the variances on the responses. The R^2 and R_{adj}^2 are 0.9544 and 0.8957, which implies the quadratic polynomial equation model above could fit well with the experiment values. Also, the interactive term coefficients (X_1 X_2) are significant, which showed the interaction existed between aqueous phase velocity and ultrasound power.

3.8 Analysis of response surfaces

Both the response surface plots and the contour plots illustrate the interaction between independent variance on extraction efficiency. As shown in Figure 7a, the efficiency increased as aqueous phase velocity decreased when ultrasound power was 0 W, and high extraction efficiency was found only at low aqueous phase velocity. However, when ultrasound power gradually increased, the curve of the extraction efficiency over the aqueous phase was flattened by the increasing ultrasound power. The higher extraction efficiency was also shown in the contour plot when aqueous phase velocity was high. In summary, the ultrasound power had covered the defect of short residence time brought by high aqueous phase velocity, and the interaction between the two factors had a significant influence on extraction efficiency (p<0.05). Also, From Figure 7b, the extraction efficiency increased as aqueous phase velocity decreased or O/A ratio increased. A high O/A ratio and slow velocity could positively influence the efficiency. The response surface plot can be combined with the fitting model to reach a conclusion, which was aqueous phase velocity and O/A ratio significantly affected the efficiency (p<0.01). In Figure 7c, the extraction efficiency increased as both parameters increased. This means ultrasound power and O/A ratio had a positive effect on the extraction efficiency. However, the

interaction between aqueous phase velocity and O/A, ultrasound power and O/A was not significant according to the results obtained above (p>0.05).

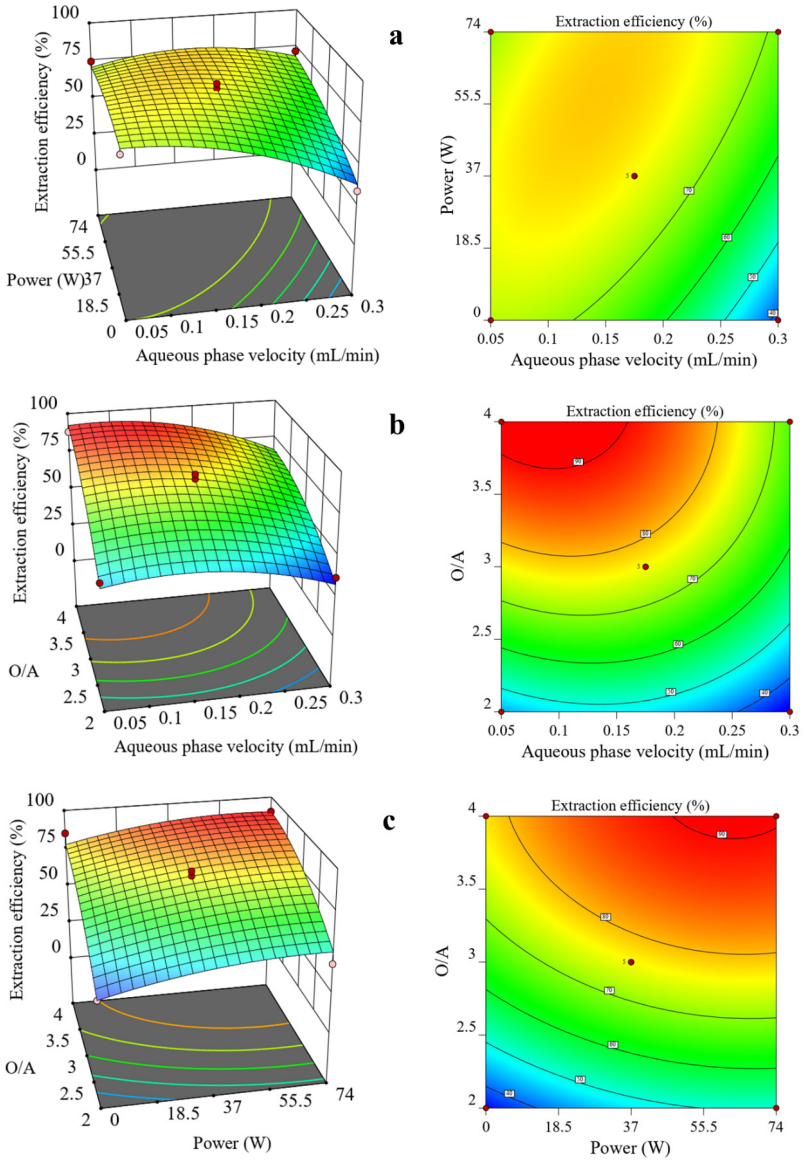

Figure 7. Response surface plots and contour plots of three variance interaction on extraction efficiency (a) Aqueous phase velocity and ultrasound power, O/A ratio = 3; (b) Aqueous phase velocity and O/A ratio ultrasound power = 37 W; (c) Ultrasound power and O/A ratio; aqueous phase velocity = 0.175 mL/min.

3.9 Recycle of PN-1

To investigate the reuse of the extractant, the stripping process of the extractant was studied in a mechanical shaker with conical flasks. The organic phase loaded with magnesium (average concentration of 2.45 g/L) was stripped using 1 mol/L H_2SO_4 solution at different phase ratios with a stripping time of 20 min.

The result in Figure 8 shows that stripping efficiency almost reached 100% with phase ratios less than 2 and decreased with the increasing phase ratio. The high efficiency of the stripping process could be understood as the H^+ quickly replaced the Mg^{2+} cations, which indicates that the stability sequence of the extracted complex was HR > MgR_2, and it is consistent with the sequence described in Section 3.1. Moreover,

under an O/A ratio of 2, the stripped organic phase was reused to extract Mg^{2+}. The result in Figure 9 shows it is still maintained to some extent of extraction ability.

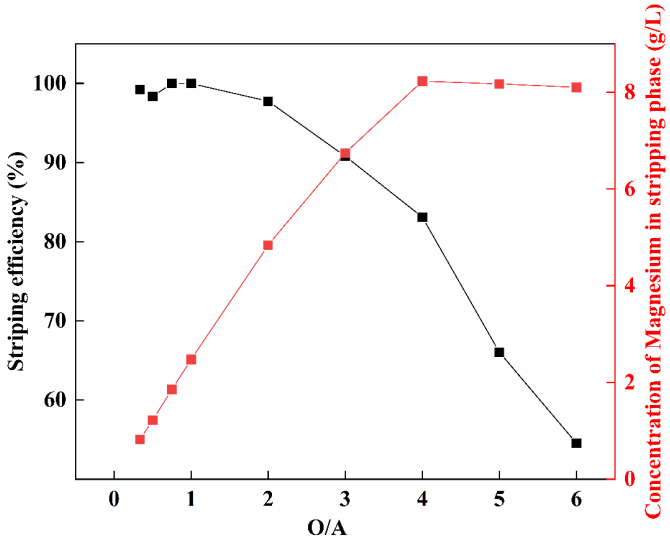

Figure 8. Stripping efficiency of Mg^{2+} using 1 mol/L H_2SO_4.

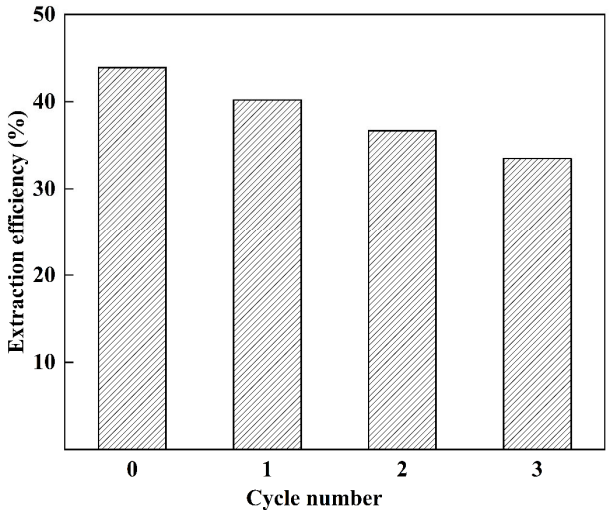

Figure 9. Recycle of the extractant.

4. Conclusion

The UAME system for the extraction of magnesium from WPA had been developed using a new extractant PN-1 synthesized by ourselves. In UAME, the extraction efficiency of 88.84% was obtained at 0.05 mL/min aqueous phase velocity under an O/A ratio of 4 without ultrasound. The extraction speed had significantly improved when ultrasound was introduced into the extraction system. The results show that at 0.2 mL/min aqueous phase velocity, the efficiency could also reach 89.09% with O/A ratio of 4 and ultrasound power of 74 W.

The RSM result indicates that O/A ratio and aqueous phase velocity were the two most significant parameters, and the interaction between aqueous phase velocity and ultrasound power also significantly influenced extraction efficiency. The stripping process shows that an average of 98% of Mg^{2+} could be stripped, and the new extractant PN-1 has medium reusability. Hence, utilizing the UAME method and PN-1 extractant could be a promising way to remove Mg^{2+} ions from WPA.

Supporting Information

The Supporting Information is available free of charge at https://doi.org/10.15261/serdj.29.9.

Acknowledgments

We much acknowledge the help from the school of chemical engineering, Sichuan University, for providing the equipment and reagents.

References

1) H. M. Abdel-Ghafar, E. A. Abdel-Aal, M. A. M. Ibrahim, H. El-Shall, A. K. Ismail, *Hydrometallurgy*, **184**, 1-8 (2019).
2) X. Lv, D. Liu, J. Ji, J. Chen, T. Yang, *Solvent Extr. Res. Dev., Jpn.*, **24**, 11-22 (2017).
3) S. Zhang, X. Lv, Q. Xia, J. Zhang, J. Chen, D. Liu, *Solvent Extr. Res. Dev., Jpn.*, **26**, 51-62 (2019).
4) J. Yu, D. Liu, *Chem. Eng. Res. Des.*, **88**, 712-717 (2010).
5) W. Cate, M. Deming, *J. Chem. Eng. Data*, **15**, 290-295 (1970).
6) M. I. El-Khaiary, *Sep. Purif. Technol.*, **12**, 13-16 (1997).
7) W. P. Thomas, W. S. Lawton. '*Stable ammonium polyphosphate liquid fertilizer from merchant grade phosphoric acid*', US Patent 4,721,519 (1988).
8) S. G. Whitney, W. R. Erickson. '*Method of selectively removing adsorbed calcium and magnesium from cation exchange resins*', US Patent 4,363,880 (1982).
9) Q. Nan, P. Li, B. Cao, *Appl. Surf. Sci.*, **387**, 521-528 (2016).
10) X. Li, C. Zhang, S. Zhang, J. Li, B. He, Z. Cui, *Desalination*, **369**, 26-36 (2015).
11) M. Gonzalez, R. Navarro, I. Saucedo, M. Avila, J. Revilla, C. Bouchard, *Desalination*, **147**, 315-320 (2002).
12) A. N. Baumann. '*Separation of dissolved substances from wet process phosphoric acid*', US Patent 4,640,828 (1987).
13) H. N. Hedrick, S. G. Whitney. '*Method of using higher concentration sulfuric acid for stripping and precipitation of adsorbed magnesium*', US Patent 4,493,907 (1985).
14) N. S. Awwad, Y. A. El-Nadi, M. M. Hamed, *Chem. Eng. Process.*, **74**, 69-74 (2013).
15) R. Kijkowska, D. Pawlowska-Kozinska, M. J. Z. Kowalski, Z. Wzorek, *Sep. Purif. Technol.*, **28**, 197-205 (2002).
16) Y. Wang, L. Zeng, G. Zhang, W. Guan, Z. Sun, D. Zhang, J. Qing, *Hydrometallurgy*, **185**, 55-60 (2019).
17) E. Jang, Y. Jang, E. Chung, *Appl. Geochem.*, **78**, 343-350 (2017).
18) G. Ye, Y. Hu, X. Tong, L. Lu, *Hydrometallurgy*, **177**, 27-33 (2018).
19) Y. Yang, Z. Wang, D. Hu, K. Xiao, J.-Y. Wu, *Food Hydrocolloids*, **79**, 189-196 (2018).

20) Y. Tao, D. Wu, Q. A. Zhang, D. W. Sun, *Ultrason. Sonochem.*, **21**, 706-715 (2014).
21) S. Both, F. Chemat, J. Strube, *Ultrason. Sonochem.*, **21**, 1030-1034 (2014).
22) J. Azmir, I. S. M. Zaidul, M. M. Rahman, K. M. Sharif, A. Mohamed, F. Sahena, M. H. A. Jahurul, K. Ghafoor, N. A. N. Norulaini, A. K. M. Omar, *J. Food Eng.*, **117**, 426-436 (2013).
23) D. Horžić, A. R. Jambrak, A. Belščak-Cvitanović, D. Komes, V. Lelas, *Food Bioprocess Technol.*, **5**, 2858-2870 (2012).
24) A. DiNardo, J. Subramanian, A. Singh, *Sep. Sci. Technol.*, **55**, 523-536 (2019).
25) D. M. Roberge, L. Ducry, N. Bieler, P. Cretton, B. Zimmermann, *Chem. Eng. Technol.*, **28**, 318-323 (2005).
26) Y. He, J. Pei, C. Srinivasakannan, S. Li, J. Peng, S. Guo, L. Zhang, S. Yin, *Hydrometallurgy*, **179**, 175-180 (2018).
27) J. Kobayashi, Y. Mori, K. Okamoto, R. Akiyama, M. Ueno, T. Kitamori, S. Kobayashi, *Science*, **304**, 1305-1308 (2004).
28) M. Maeki, Y. Hatanaka, K. Yamashita, M. Miyazaki, K. Ohto, *Solvent Extr. Res. Dev., Jpn.*, **21**, 77-82 (2014).
29) W. E. TeGrotenhuis, R. J. Cameron, M. G. Butcher, P. M. Martin, R. S. Wegeng, *Sep. Sci. Technol.*, **34**, 951-974 (1999).
30) M. Miyazaki, Y. Yamaguchi, T. Honda, H. Maeda, *Open Chem. Eng. J.*, **5**, 13-17 (2011).
31) R. G. Parr, R. G. Pearson, *J. Am. Chem. Soc.*, **105**, 7512-7516 (1983).
32) R. G. Pearson, *J. Chem. Educ.*, **45**, 581-587 (1968).
33) D. Shi, B. Cui, L. Li, M. Xu, Y. Zhang, X. Peng, L. Zhang, F. Song, L. Ji, *Desalination*, **479**, 114306 (2020).